Available online at www.sciencedirect.com

ScienceDirect

Procedia CIRP 113 (2022) 417–421

www.elsevier.com/locate/procedia

ISEM XXI

Experimental setup for the investigation of the transport of different gas bubble sizes during electrochemical machining based on similarity theory using particle image velocimetry

E. Tchoupe[a,*], L. Heidemanns[a], A. Klink[a], T. Herrig[a,b], M. Klaas[c], D. Lauwers[c], W. Schröder[c]

[a] *Laboratory for Machine Tools and Production Engineering (WZL) of RWTH Aachen University, Campus-Boulevard 30, Aachen 52074, Germany*
[b] *Fraunhofer Institute for Production Technology IPT, Steinbachstraße 17, 52074 Aachen, Germany*
[c] *Chair of Fluid Mechanics and Institute of Aerodynamics (AIA), RWTH Aachen University, Wüllnerstr. 5a, 52062 Aachen, Germany*

* Corresponding author. Tel.: +49 241 80 28073; *E-mail address:* e.tchoupe_sambou@wzl.rwth-aachen.de

Abstract

The major advantage of electrochemical machining (ECM) is the ability to machine materials regardless of their mechanical properties such as hardness or temperature resistance. This property of the ECM process makes it ideal for processing difficult-to-machine materials such as high-performance nickel-based alloys and single-crystal alloys. However, it is difficult to predict a priori the appropriate tool electrode for a given workpiece contour. This is not only due to the constantly changing properties of the electrolyte during machining, but also to the transient nature of the working gap. To simplify tool design in ECM, a better understanding of the various phenomena that occur, such as gas formation and its propagation in the working gap, is necessary. This paper presents an experimental investigation of the transport of different gas bubble sizes during ECM by up-scaling the working gap according to the principles of similarity theory. The multiphase flow is analyzed using 3D particle image velocimetry, which will serve for validation of future simulation models.

Keywords: Electrochemical machining; Particle Image Velocimetry; Similarity approach;

1. Introduction

Electrochemical machining (ECM) allows efficient machining of high-strength materials, such as nickel-based alloys, while ensuring high surface quality and no thermally or mechanically damaged rim zone in agreement with McGough and Rajurkar et al. [1,2]. Therefore, it is often used for the production of turbine components such as blades as reported by Klocke et al. and Reed [3,4]. However, its high economic potential is hampered by the time-consuming and costly development of tool geometries. According to Kunieda et al. to enhance the efficiency of such a process, numerical simulation-based approaches are used to reduce the number of experimental iterations [5]. Such a model was developed and successfully validated at the WZL by Klocke et al. and Zeis [6–8]. In ECM, the tool is fed under steady state conditions at the same rate at which the workpiece dissolves so that the electrode gap remains constant. As the tool geometry is fixed, the equilibrium-working gap determines final geometry of the workpiece (Fig. 1). Therefore, for a target geometry the tool is designed based on the prediction of the equilibrium-working gap. The size of this gap is directly linked to the electrolyte conductivity. Concerning the later, it depends on the process byproducts such as heat and hydrogen bubbles. Whereas high temperatures caused by Joule heating increase the conductivity of the electrolyte, a high hydrogen content achieves quite the opposite effect. However, they both increase downstream as the electrolyte is pumped to flush

10.1016/j.procir.2022.09.193

them out of the working gap. Consequently, the local electrolyte conductivity and hence the local interelectrode gap vary in the direction of the electrolyte flow. In accordance with Hopenfeld, the challenge in the ECM tool design process is therefore the ability to predict these variations for a given set of operating conditions [9]. A costly iterative process often compensates for this such that ECM is mostly used in productions with large batch sizes [3].

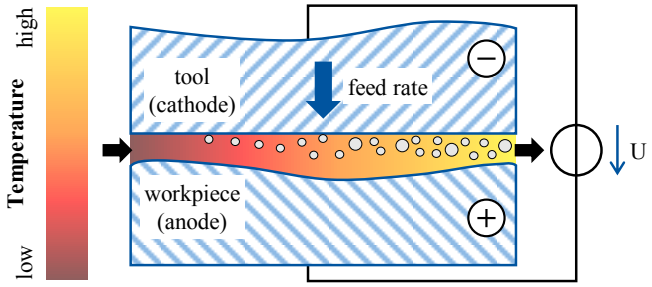

Fig. 1: Material removal principle of electrochemical machining based on [6]

In the following, several studies that investigate the gap phenomena in order to simplify tool development in ECM are presented. As mentioned above the use of simulation results of the ECM process has shown great potential in the prediction of the machining gap variation [5]. However, acceptable simulation results require adequate boundary conditions. To address this, Klocke et al. used a high-speed camera and thermography camera system to visualize the working gap phenomena [6]. A special arrangement with industrially relevant ECM conditions for this purpose was set up. Furthermore, their findings were used as input and validation of an interdisciplinary process simulation model based on the conservation equations. The results showed excellent accordance between the simulation and experimental results. Nevertheless, the simulation model was limited to a 2D geometry. Similarly, 2D simulations of the electrolyte flow in narrow openings during electrochemical machining were carried out by Klink et al. [10].

Much earlier, Hopenfeld et al. also analyzed the gas-electrolyte mixture using conservation laws [9]. For this, they assumed that the gas bubbles and the electrolyte form a perfect homogeneous mixture and have the same velocities. While their numerical results could predict quite accurately the trends of the conductivity of the electrolyte-gas mixture, they however could not formulate precise values for this. Tsuboi et al. investigated the behavior of hydrogen bubbles in the working gap [11]. They calculated the trajectories of the bubbles and analyzed their distribution in a 3D model for a compressor blade based on the assumption that the bubbles are of negligible weight and do not affect the fluid. For their target geometry, they could determine the regions where bubbles had high resident times. However, they did not relate these results to process variables like the material removal rate (MRR) or the local interelectrode gap. Boiling of the electrolyte caused by Joule heating often results in the formation of vapor bubbles. Shimasaki et al. analyzed this phenomenon for a setup with stationary electrodes [12]. For observation purposes, they used transparent electrodes. While they mostly consider bubbles formed because of boiling of the electrolyte, bubbles resulting from the chemical decomposition of the electrolyte are not considered. Moreover, machining was carried out with a stationary electrolyte, which is rarely used industrially. Saxena et al. used large scale particle image velocimetry to perform in-situ visualization of the working gap of the hybrid laser-electrochemical micromachining [13]. This approach, which is of high potential, was mainly used to generate better understandings of the hybrid laser-electrochemical micromachining process.

From the above-described literature, it is clear that there are still some phenomena occurring in the interelectrode gap that have not been fully investigated or investigated with all influencing factors such as the multiphase flow field in 3D. Concerning the hydrogen propagation, it in turns depends among others on the flushing configuration (volume flow rate, etc.) and must be addressed. This paper presents an in-situ measurement approach of these phenomena. Considering the constraints imposed by its small nature, the working gap will be enlarged according to the principle of similarity theory which is based on Reynolds Number as suggested by Rommes et al. [14]. Measurements here are performed by optical means such as Particle Image Velocimetry (PIV), which is known to possess high spatial and temporal resolutions in line with Raffel et al. [15]. Such knowledge is inescapable for the development of an efficient modeling approach that can define the necessary operating parameters for an end-shape based on a given initial geometry using ECM and its variants (Fig. 2).

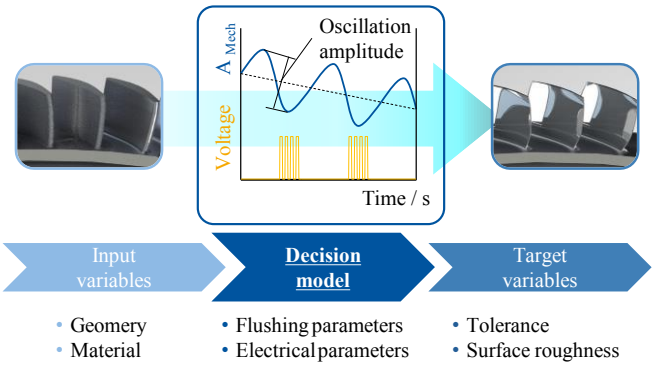

Fig. 2: Concept of the decision model as suggested by Rommes et al. [16]

2. Theoretical background

In ECM, most of the phenomena that occur in the working gap strongly depend on the local hydrodynamic conditions. Therefore, proper understanding of the ECM process can hardly be achieved without profound understanding of the flow properties. Owing to its small nature (working gaps of 0.05 to 0.5 mm), analysis of the flow of a typical ECM process is challenging. In order to circumvent this limitation, Rommes et al. proposed a novel concept for the investigation of the gap phenomena by up-scaling the working gap [16]. Scaling is based on the principle that two fluid flows will be identical if they have similar setups (similar shapes with different sizes) with identical boundary conditions and the same Reynolds number (similarity theory) [14]. The latter, which is the ratio of inertial to viscous forces of the flow, depends on the fluid's material parameters. Up-scaling the gap allows access for a suitable light source and cameras such

that the instantaneous flow field of the electrolyte can be analyzed using PIV measurements.

Given the requirements of this measurement approach, a convenient working gap of about 10 mm is required, which corresponds to an up-scaled factor of about 100 of the actual ECM working gap. In accordance with the principle of similarity theory, the velocity of the electrolyte must be reduced by the same factor to keep the Reynolds number constant. Regarding the Reynolds number, this is chosen in the range of $750 < Re < 12{,}000$, which corresponds to reduced velocities in the range of 0.075 to 1.2 m/s. As for hydrogen gas bubbles with typical diameters in the range of 0.001 - 0.01 mm, they must be increased for the up-scaled setup to 0.1 - 1 mm while the pressure drop must be reduced. Table 1 shows a summary of the typical ECM process parameters and that for the up-scaled setup. Hydrogen bubbles that result from electrolysis in the real process cannot be realized in the same way for the up-scaled setup because of the required electrical power. In order to keep the ratio of the constituents of the multiphase flow identical to the real process, similar current densities are needed. Consequently, very large electrical currents would be required with respect to the up-scaled configuration. However, for specific analysis small electrodes can be used with corresponding electrical power. Tchoupe et al. have already proposed and validated a seeding mechanism for gas bubbles of the required diameter that can be used as a substitute for electrolysis [17].

Table 1. Real process and optimized experimental parameters (up-scaled setup)

Process parameters	Real process	Experimental values
Working gap / (mm)	0.1	10
Flow velocity / (m/s)	15 - 50	0.075 - 1.2
Flow rate / (l/min)	0.45 - 15	45 - 1,500
Bubble diameter / (mm)	0.001 - 0.01	0.1 - 1
Pressure drop / (bar/m)	200	$2 \cdot 10^{-4}$

3. Experimental setup

Fig. 3 shows a constructed and built prototype of the test bench. With a reduced length of 1.5 m the volume flow rate, which is the main variable, is to be controlled based on the inlet pressure. Simple estimates showed that a pressure loss of 0.3 bar occurs over the length of the channel at an ECM-typical Reynolds number of $Re = 7500$. Taking into account the hydrostatic pressure of the fluid within the inlet tank, this pressure difference is realized by a water level of about 30 cm above the channel inflow [16]. However, initial trials revealed that maintaining a given height is challenging such that an alternative means to control the flow was necessary.

Fig. 4 shows the improved test bench for the investigation of the hydrogen evolution during machining in ECM. The test channel with a width of 200 mm yields an aspect ratio of 20:1 with respect to the height of the working gap. Moreover, the total length of the test canal of 2 m with 1.2 m run before gas is seeded ensures that a fully developed flow is achieved. As for the gas bubbles, their quantity as well as their sizes can be varied. The walls of the test canal are made up of acrylic plates, which provide good optical access to the flow. Metal bars between the plates are used to keep the height of the channel constant.

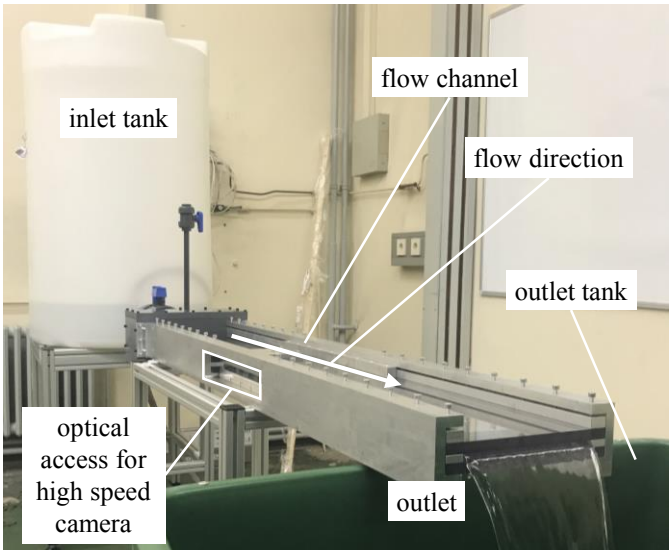

Fig. 3: Prototype of the channel flow facility

A submersible pump drives the flow. Using a potentiometer, the electric voltage supplied to the pump is varied and therefore used to control the volume flow rate and hence the velocity of the electrolyte with much more simplicity and ease. The potentiometer is varied until the target volume flow rate is read on the rotameter. The fluid from the rotameter passes through a honeycomb structure which improves the flow uniformity in harmony with Durst et al. and Niederschulte et al. [18,19]. The flow channel is preceded by nozzle, which ensures a smooth transition from the circular to rectangular profile over a total length of 400 mm.

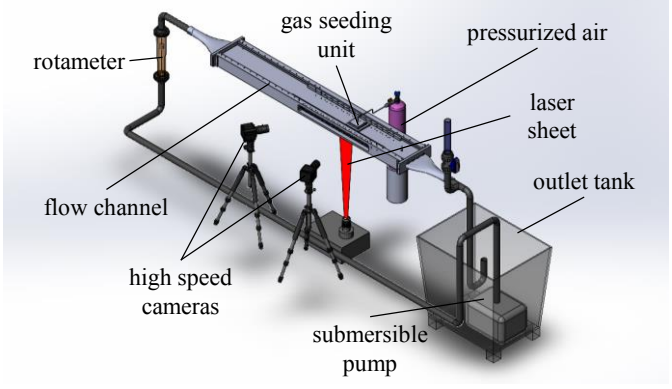

Fig. 4: Conceptual design of the improved test bench

An aeration duct ensures complete elimination of trapped gas bubbles in the setup when starting the pump. In order to control the gas bubbles in the test canal, they must be extirpated at the end of the canal. This is achieved by placing the pump at a distance from the U-tube (Fig. 4). Temperature variations are readily implemented by inserting a water heater equipped with a thermostat.

The conductivity of electrolyte-gas bubble mixture is sensitive not only to temperature, but also to the ratio of the different constituents. As for the later, analytical methods for its investigation have being proposed by McGough and Thorpe et al. [1,20] but have hardly been validated due to the small working gap. With the current experimental setup, such models can now readily be validated. Fig. 5 shows an approach for the investigation of the influences of the gas transport in the working gap on the electrical conductivity of the multiphase flow. While the gas volume, which is seeded into the test channel at a known rate, is measured by optical means, the conductivity of the mixture is determined using the 'contact electrode cell' approach as described by Otterson [21]. The application of an alternating voltage to the electrodes causes the ions in the fluid to be 'excited'. As a result, an alternating 'ionic current' can be measured. Using Ohms law to determine the resistance of the electrolytic path the conductance, which is the reciprocal of the resistance, can be formulated.

Although the cell constant, which is the ratio of the surface area of the electrodes to the distance between them, describes the geometry of the conductivity cell it is rarely derived from measured dimensions. Instead, the cell constant is determined based on the conductivity (S/m) measurement using a calibrated instrument and the conductance from the conductivity cell (S). Their ratio is the cell constant [21].

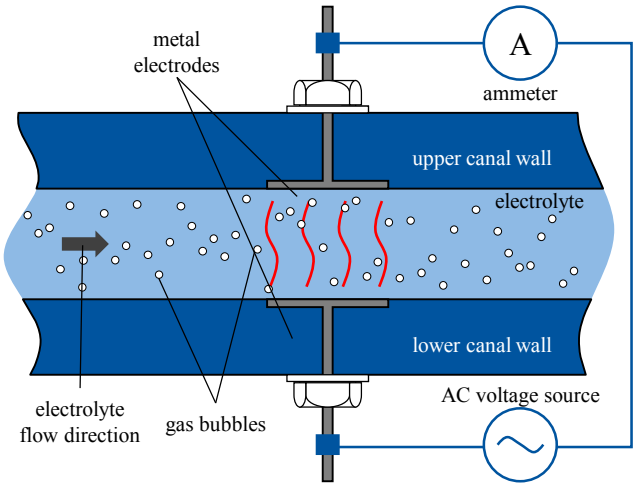

Fig. 5: Electrolyte conductivity measurement approach

4. PIV measurements of proposed experimental setup

The main objective of the proposed setup is to develop a better understanding of the ECM process and to validate the simulations. On the one hand, the influence of different factors such as temperature and hydrogen bubbles on the conductivity of the electrolyte can be fully analyzed, and on the other hand, different simulation approaches of the process and its variants, not validated so far in congruence with Bergs et al. and Klocke et al. [22,23], can be realized. Be it the size and shape of the bubbles or the velocity components of the flowing electrolyte, this can be measured with high temporal and spatial resolutions by optical means such as Particle Image Velocimetry.

In order to validate the feasibility of this measurement method, preliminary experiments were performed on a similar test bench. These experiments were carried out in a horizontal channel facility with a width of 200 mm and a channel height of h = 10 mm. The aspect ratio of the channel is 20:1, which guarantees a homogeneous mean flow distribution upstream of the test section and the gas bubble inlet. While the channel sidewalls are made of aluminum with Perspex inlets, the top and bottom walls are made of Perspex plates, providing optical access in the horizontal and vertical direction. A fully developed turbulent flow in the test section is provided by an inlet with a length of 1.000 mm, i.e., 100 channel heights.

Fig. 6 shows the local mean velocity profiles for several streamwise positions varying from X / h = 98 to 107 upstream of the test section and along the center line Y / h = 0 of a channel facility with aspect ratio of 20:1. The measurements were performed for a bulk Reynolds number of Re = 6,600 based on the channel height h using 2D/2C PIV. For comparison, the direct numerical simulation (DNS) results of Moser et al. [24] are also included in the plot. Note that the computations were carried out for a slightly different bulk Reynolds number of Re = 5,800. The experimental data of the channel flow facility and the DNS results collapse very well, evidencing the excellent agreement of the PIV measurements with the data from the literature.

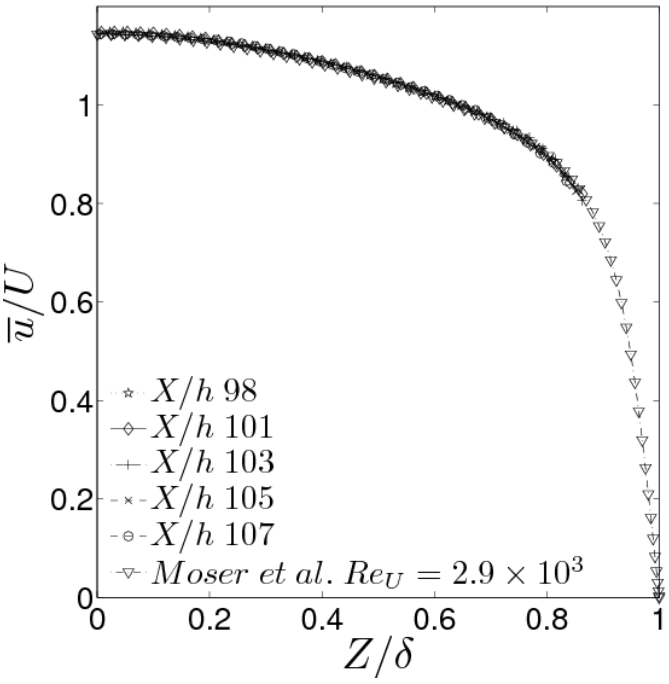

Fig. 6: Normalized mean velocity profiles upstream of the test section of a 20:1 channel for a bulk Reynolds number of Re=6.600 measured with PIV in comparison to numerical results of Moser et al. [24]

Fig. 7 shows a comparison of the measured root-mean-square (rms) values of the fluctuation of the Cartesian velocity components at X/h = 103 for a bulk Reynolds number of Re = 6,600 with the corresponding DNS results of Moser et al. at Re = 5,800, evidencing the fully turbulent flow of such a channel facility upstream of the test section [24].

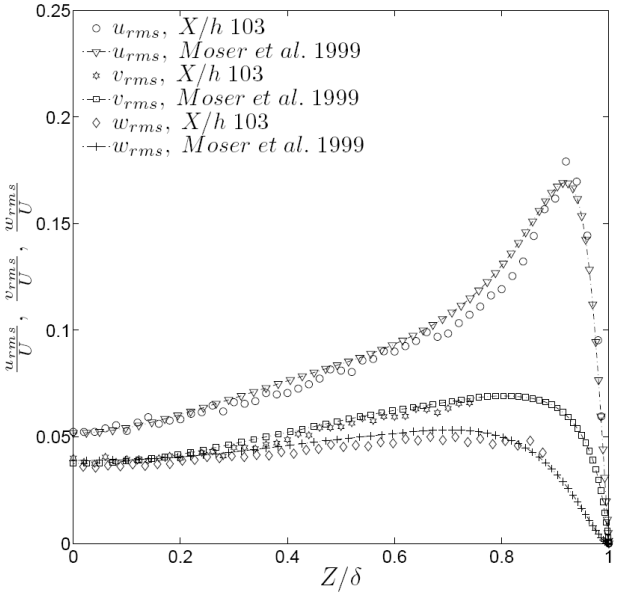

Fig. 7: Normalized root-mean-square velocity fluctuations at Re = 6,600 in comparison with DNS data at Re = 5,800 of Moser et al. [24]

5. Summary and outlook

An experimental setup for the study of the gap phenomena during the ECM process is presented. The setup enables different aspects of the process such as hydrogen bubble transport to be analyzed. Based on the contact electrode cell approach, a method is presented for an investigation of the influences of bubble sizes as well as flushing velocity and temperature on the conductivity of the electrolyte. Moreover, the suitability of PIV measurements based on a similar setup showed good agreement with the numerical results. Similarly, this approach can be used to validate forthcoming numerical methods. In the future, the setup will be extended to include movable walls that allow interaction between the liquid structure of the electrolyte and the workpiece.

Acknowledgements

The authors would like to thank the German Research Foundation Priority Program SPP2231-FLUSIMPRO “Simulation of the pulsed electrochemical machining (PECM) of thin-walled workpieces for turbomachinery component manufacture - SIMPECT”, project number 439915866, for funding this research.

References

[1] McGeough, J.A., 1974. Principles of electrochemical machining. Chapman and Hall, London.
[2] Rajurkar, K.P., Kozak, J., Wei, B., McGeough, J.A., 1993. Study of Pulse Electrochemical Machining Characteristics. CIRP Annals 42 (1), 231–234.
[3] Klocke, F., Klink, A., Veselovac, D., Aspinwall, D.K., Soo, S.L., Schmidt, M., Schilp, J., Levy, G., Kruth, J.-P., 2014. Turbomachinery component manufacture by application of electrochemical, electro-physical and photonic processes. CIRP Annals 63 (2), 703–726.
[4] Reed, R.C., 2006. The Superalloys. Cambridge University Press, Cambridge.
[5] Hinduja, S., Kunieda, M., 2013. Modelling of ECM and EDM processes. CIRP Annals 62 (2), 775–797.
[6] Klocke, F., Zeis, M., Herrig, T., Harst, S., Klink, A., 2014. Optical in Situ Measurements and Interdisciplinary Modeling of the Electrochemical Sinking Process of Inconel 718. Procedia CIRP 24, 114–119.
[7] Klocke, F., Zeis, M., Klink, A., 2015. Interdisciplinary modelling of the electrochemical machining process for engine blades. CIRP Annals 64 (1), 217–220.
[8] Zeis, M., 2015. Modellierung des Abtragprozesses der elektrochemischen Senkbearbeitung von Triebwerksschaufeln. Zugl.: Aachen, Techn. Hochsch., Diss., 2015, 1. Aufl. ed. Apprimus-Verl., Aachen, 131 pp.
[9] Hopenfeld, J., Cole, R.R., 1969. Prediction of the One-Dimensional Equilibrium Cutting Gap in Electrochemical Machining. Journal of Engineering for Industry 91 (3), 755–763.
[10] Klink, A., Heidemanns, L., Rommes, B., 2020. Study of the electrolyte flow at narrow openings during electrochemical machining. CIRP Annals 69 (1), 157–160.
[11] Tsuboi, R., Yamamoto, M., 08102008. Investigating Behavior of Hydrogen Bubbles in Electro-Chemical Machining, in: Volume 1: Symposia, Parts A and B. ASME 2008 Fluids Engineering Division Summer Meeting collocated with the Heat Transfer, Energy Sustainability, and 3rd Energy Nanotechnology Conferences, Jacksonville, Florida, USA. 10.08.2008 - 14.08.2008. ASMEDC, pp. 275–283.
[12] Shimasaki, T., Kunieda, M., 2016. Study on influences of bubbles on ECM gap phenomena using transparent electrode. CIRP Annals 65 (1), 225–228.
[13] Saxena, K.K., Chen, X., Vetrano, M.R., Qian, J., Reynaerts, D., 2020. Real-time on-machine observations close to interelectrode gap in a tool-based hybrid laser-electrochemical micromachining process. Sci Rep 10 (1).
[14] Rommes, B., Klink, A., Herrig, T., Vorspohl, J., Ehle, L., Bergs, T., 2020. Formation of Flow-Grooves during Electrochemical Machining, in: 16th International Symposium on Electrochemical Machining Technology INSECT Proceedings. November 24-25, 2020. Verlag Wissenschaftliche Scripten, Auerbach, pp. 27–32.
[15] Raffel, M., Willert, C.E., Scarano, F., Kähler, C.J., Wereley, S.T., Kompenhans, J., 2018. Particle Image Velocimetry. Springer International Publishing, Cham.
[16] Rommes, B., Lauwers, D., Herrig, T., Meinke, M., Schrder, W., Klink, A., 2021. Concept for the experimental and numerical study of fluid-structure interaction and gas transport in Precise Electrochemical Machining. Procedia CIRP 102, 204–209.
[17] Tchoupe, E., Heidemanns, L., Herrig, T., Klink, A., Lauwers, D., Schröder, W., 2021. Study of the multiphase electrolyte flow during electrochemical machining (ECM) using dynamic similarity, in: 17th International Symposium on Electrochemical Machining Technology INSECT 2021 Proceedings. November 25-26, 2021, pp. 15–21.
[18] Durst, F., Fischer, M., Jovanovic´, J., Kikura, H., 1998. Methods to Set Up and Investigate Low Reynolds Number, Fully Developed Turbulent Plane Channel Flows. Journal of Fluids Engineering 120 (3), 496–503.
[19] Niederschulte, M.A., Adrian, R.J., Hanratty, T.J., 1990. Measurements of turbulent flow in a channel at low Reynolds numbers. Experiments in Fluids 9 (4), 222–230.
[20] Thorpe, J.F., Zerkle, R.D., 1969. Analytic determination of the equilibrium electrode gap in electrochemical machining. International Journal of Machine Tool Design and Research 9 (2), 131–144.
[21] Otterson, D.W., 2015. Tech Talk: (10) Electrolytic Conductivity Measurement Basics. Measurement and Control 48 (8), 239–241.
[22] Bergs, T., Heidemanns, L., Klink, A., 2020. Simulation Assisted Cathode Design for the Manufacturing of Complex Geometries by Electrochemical Machining (ECM). Procedia CIRP 95, 688–693.
[23] Klocke, F., Heidemanns, L., Zeis, M., Klink, A., 2018. A Novel Modeling Approach for the Simulation of Precise Electrochemical Machining (PECM) with Pulsed Current and Oscillating Cathode. Procedia CIRP 68, 499–504.
[24] Moser, R.D., Kim, J., Mansour, N.N., 1999. Direct numerical simulation of turbulent channel flow up to Re_τ=590. Physics of Fluids 11 (4), 943–945.